

Finite-time Scaling beyond the Kibble-Zurek Prerequisite: Driven Critical Dynamics in Strongly Interacting Dirac Systems

Zhi Zeng^{1,2,*}, Yin-Kai Yu^{1,2,*}, Zhi-Xuan Li^{1,2,*}, Zi-Xiang Li^{3,4,†} and Shuai Yin^{1,2,‡}

¹Guangdong Provincial Key Laboratory of Magnetoelectric Physics and Devices,

School of Physics, Sun Yat-Sen University, Guangzhou 510275, China

²School of Physics, Sun Yat-Sen University, Guangzhou 510275, China

³Beijing National Laboratory for Condensed Matter Physics & Institute of Physics,
Chinese Academy of Sciences, Beijing 100190, China and

⁴University of Chinese Academy of Sciences, Beijing 100049, China

(Dated: March 29, 2024)

In conventional quantum critical point (QCP) characterized by order parameter fluctuations, the celebrated Kibble-Zurek mechanism (KZM) and finite-time scaling (FTS) theory provide universal descriptions of the driven critical dynamics. However, in strongly correlated fermionic systems where gapless fermions are usually present in vicinity of QCP, the driven dynamics has rarely been explored. In this Letter, we investigate the driven critical dynamics in two-dimensional Dirac systems, which harbor semimetal and Mott insulator phases separated by the QCP triggered by the interplay between fluctuations of gapless Dirac fermions and order-parameter bosons. By studying the evolution of physical quantities for different driving rates through large-scale quantum Monte Carlo simulation, we confirm that the driven dynamics is described by the FTS form. Accordingly, our results significantly generalize the KZM theory by relaxing its requirement for a gapped initial state to the system accommodating gapless Dirac fermionic excitation. Through successfully extending the KZM and FTS theory to Dirac QCP, our work not only brings new fundamental perspective into the nonequilibrium critical dynamics, but also provides a novel theoretical approach to fathom quantum critical properties in fermionic systems.

Introduction— Fathoming nonequilibrium universal properties near a quantum critical point (QCP) is one of the central issues in modern physics [1–4]. Although the general organizing principle for the nonequilibrium critical dynamics is still elusive, a unified framework for understanding the generation of topological defects after the linear quench was proposed by Kibble in cosmological physics and then generalized by Zurek in condensed matter systems [5, 6]. This celebrated Kibble-Zurek mechanism (KZM) has aroused intensive investigations from both theoretical and experimental aspects, exerting far-reaching significance in both classical and quantum phase transitions [5–36]. More interestingly, it was found that scaling behaviors can also manifest themselves in the whole driven process [37–42]. As a generalization of the KZM, a finite-time scaling (FTS) theory was proposed to systematically understand the full scaling properties [43, 44]. These full scaling forms have been verified in various systems from numerical to experimental works [30, 31, 41, 43–54]. Moreover, the KZM and the FTS recently show their fabulous power in state preparations and probing critical properties in fast-developing programmable quantum devices [30, 31, 52–55].

The fermionic QCP [56–65], in which gapless fermionic excitations are present in vicinity of the transition point, are ubiquitous to strongly correlated quantum materials such as heavy-fermion systems [66–70], cuprate and Fe-based superconductors [71–76], and twisted bilayer graphene [77–80]. In the aspects of equilibrium nature, many intriguing phenomena are unveiled arising from the interplay between critical fluctuations of order parameter

and gapless fermions, including strange metallic transport [81–85], high- T_c superconductivity [86–90] and intertwined ordering [91–97]. In contrast, the nonequilibrium properties of quantum driven dynamics in fermionic QCP are largely unaddressed.

The QCP occurring in Dirac semimetal (DSM), dubbed as Dirac QCP, represents a typical class of fermionic QCP. The studies of Dirac QCP stem from the research in modern high-energy physics, such as chiral symmetry in QCD and mass generation via spontaneously symmetry breaking [98–104]. From the perspectives of statistical mechanics and condensed matter physics, Dirac quantum criticality also attracts enormous attentions, particularly after the experimental realization of two-dimensional Dirac fermions in graphene and various topological insulators or semimetals. The presence of Dirac fermions is theoretically revealed to tremendously enrich quantum critical properties, rendering novel universal classes of quantum phase transition without classical counterpart [105–150]. Consequently, fathoming the nonequilibrium driven dynamics in Dirac QCP has overarching meaning in basic theory, as well as immediate applications in the context of detecting and exploring fermionic QCP in experimental platform including realistic materials and quantum devices [151–153]. Particularly, whether the original KZM is still applicable in the presence of gapless fermions remains largely elusive, constituting a fundamental question that bears profound impact on the theory of phase transition and nonequilibrium physics.

However, directly attacking the real-time dynamics in two or higher spatial dimension is largely hindered by the

lack of reliable theoretical or numerical methods. Specifically, quantum Monte Carlo (QMC) fails as a result of the notorious sign problem [154–156], while the tensor-network method still needs tremendous improvements despite remarkable progress in recent years [157, 158]. Fortunately, scaling analysis demonstrates that both real- and imaginary-time driven dynamics share the same scaling form [159–161]. This inference has been verified in various systems [51, 157, 161], and particularly, substantiated by the remarkable consistency between the imaginary-time scaling and the annealing experiments in quantum devices [48, 52], bridging the gap between the QMC imaginary-time simulations without sign problem and the real-time dynamics.

In this work, for the first time we investigate the driven critical dynamics of two representative Dirac quantum critical points, belonging to chiral Heisenberg and chiral Ising universality classes respectively, via the determinant QMC method [154]. By linearly varying the interaction strength along the imaginary-time direction to cross the QCP from both the DSM and Mott insulator phases, we uncover that for large driving rate the quantum critical dynamics is governed by the driving rate. The numerical results confirm that the whole driven process satisfies the scaling form of FTS. Hence, our study significantly generalizes the conventional KZM theory. Since DSM phase harbors gapless excitations, our results unambiguously show that the prerequisite of KZM theory that the initial state is fully gapped can be relaxed to the systems accommodating gapless Dirac fermions. In addition, our numerical simulation achieves the critical exponents of phase transition, whose values obtained in previous studies on equilibrium properties are still under debate. Our approach of QMC simulation on driven critical dynamics offers a novel theoretical tool to unravel properties of Dirac QCP. Through the innovative generalization of quantum driven critical dynamics to Dirac-fermion systems, our study not only leads to a great leap to the fundamental theory of KZM and FTS, but also contributes to a feasible approach to investigate the fermionic quantum critical phenomena in realistic platform such as quantum materials and devices.

Dynamics in chiral Heisenberg criticality— A typical model hosting QCP belonging to chiral Heisenberg universality class is the Hubbard model on the half-filled honeycomb lattice with the Hamiltonian [123–127]

$$H = -t \sum_{\langle ij \rangle, \sigma} c_{i\sigma}^\dagger c_{j\sigma} + U \sum_i \left(n_{i\uparrow} - \frac{1}{2} \right) \left(n_{i\downarrow} - \frac{1}{2} \right), \quad (1)$$

in which $c_{i\sigma}^\dagger$ ($c_{j\sigma}$) represents the creation (annihilation) operator of electrons with spin σ , $n_{i\sigma} \equiv c_{i\sigma}^\dagger c_{i\sigma}$ is the electron number operator, t is the hopping amplitude between nearest neighbor sites and set as the energy unit in the following. U is the strength of the on-site repulsive interaction. The model is absent from sign problem

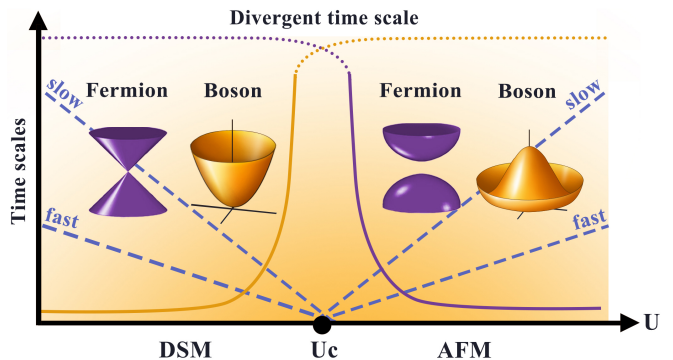


FIG. 1. Sketch of the phase diagram in Dirac systems and the protocol for driven dynamics with different initial states. The correlation time scales for both boson (yellow curve) and fermion (violet curve) are finite in one phase (solid) but divergent (dotted) in the other phase. Accordingly, the prerequisite of the original KZM that a gapped initial state should exist to protect an initial adiabatic stage, in which the transition time is larger than (dashed line) than the correlation time, breaks down.

in QMC simulation [162]. As shown in Fig. 1, a critical point U_c separates two phases. When $U > U_c$, the system is in the antiferromagnetic (AFM) Mott insulator phase in which fermions acquire a mass originating from spontaneously symmetry breaking characterized by the finite AFM order parameter $m^2 = \sum_{i,j} \eta_i \eta_j \langle S_i^z S_j^z \rangle / L^{2d}$ with $S_i^z \equiv \frac{1}{2} \mathbf{c}_i^\dagger \sigma^z \mathbf{c}_i$, $\mathbf{c} \equiv (c_\uparrow, c_\downarrow)$, and $\eta_i = \pm 1$ for $i \in A(B)$ sublattice [126, 127]. Here, L is the linear size of the system and d is the spatial dimension. In this phase, the transverse spin excitation is massless due to the presence of the Goldstone modes. In contrast, when $U < U_c$, the system is in the DSM phase with four-component massless Dirac fermion ($N_f = 2$). At U_c , both Dirac fermions and AFM order parameter bosons are gapless, giving rise to Gross-Neveu QCP belonging to chiral Heisenberg universality class [123–127].

For the driven dynamics across the critical point, based on an adiabatic-impulse-adiabatic scenario, the original KZM often requires a gapped initial state to maintain an adiabatic initial evolution [1, 2, 163], since the frozen time, which is a central notion in the KZM, lives at the edge of the adiabatic stage. After that, the KZM predicts an impulse regime wherein the system ceases evolving due to the critical slowing down [1, 2, 6]. This oversimplified assumption was further improved by the FTS theory, which demonstrated that a driven-induced time scale controls the dynamics in the impulse region and the whole evolution process can be described by the FTS forms [43–45]. Here we begin to explore whether the FTS forms are still applicable in Dirac systems with gapless initial states.

First we study the driven dynamics by varying U with imaginary time τ as $U = U_0 + R\tau$ starting from the DSM initial state with interaction strength U_0 , as illustrated in Fig. 1. We denote the distance to the critical point as g

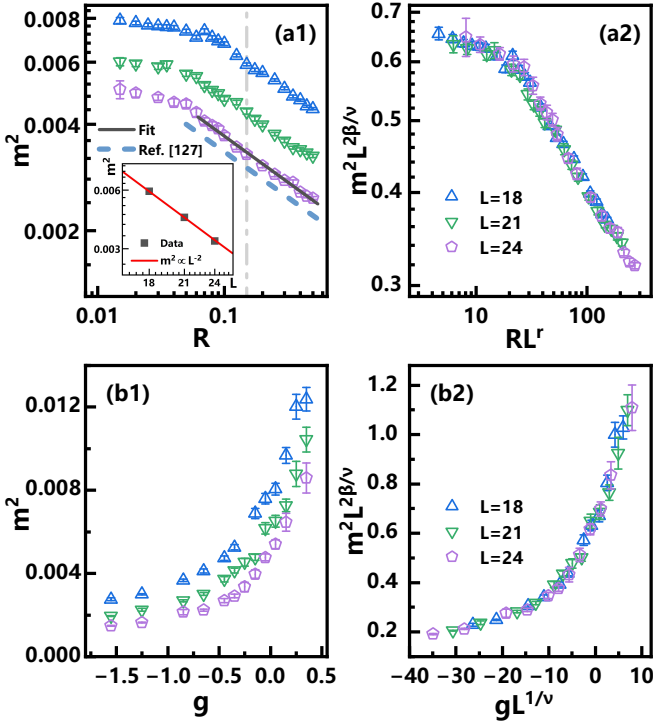


FIG. 2. Driven dynamics from the DSM phase of model (1). (a) Log-log plots of m^2 versus R for different L driven to $U_c = 3.85$ before (a1) and after (a2) rescaling. Inset in (a1) shows $m^2 \propto L^{-2}$ for $R = 0.15$ (dash-dotted line). For large R , power fitting for $L = 24$ (black solid line) shows $m^2 \propto R^{-0.26}$ with the exponent close to $(2\beta - d\nu)/\nu r = -0.257$ (dash line) from Ref. [127]. (b) Curves of m^2 versus g for fixed $RL^r = 5.41$ and different L before (b1) and after (b2) rescaling.

(Here $g = U - U_c$). When $g = 0$, from Fig. 2 (a1), we find that for large R , $m^2 \propto R^{(2\beta - d\nu)/\nu r}$ in which β and ν are the exponents for order parameter and correlation length respectively [127], and $r = z + 1/\nu$ with z the dynamic exponent. And the exponent on R is almost independent of L . In addition, for fixed R , we find that $m^2 \propto L^{-2}$. Combination of these results yields the scaling relation $m^2 \propto L^{-d} R^{(2\beta - d\nu)/\nu r}$. In contrast, when R is small, Fig. 2 (a1) shows that m^2 tends to saturate and the usual finite-size scaling $m^2 \propto L^{-2\beta/\nu}$ is restored. To reconcile these rescaling relations, the scaling form must satisfy

$$m^2(R, L, g) = L^{-d} R^{(2\beta - d\nu)/\nu r} \mathcal{F}(RL^r, gL^{1/\nu}), \quad (2)$$

in which \mathcal{F} is a non-singular scaling function and therein dimensionless quantity $gL^{1/\nu}$ is also included to take account of the off-critical-point effects. Eq. (2) is consistent with the FTS in conventional bosonic QCP [45, 46].

To confirm Eq. (2), we find that the Eq. (2) yields the scaling form $m^2 = L^{-2\beta/\nu} \mathcal{F}(RL^r, 0)$ with fixing $g = 0$. Here, we rescale m^2 and R as $m^2 L^{2\beta/\nu}$ and RL^r respectively, and reveal that the rescaled curves collapse well into a single curve, as shown in Fig. 2 (a2). The results of data collapse not only confirm Eq. (2) at $g = 0$, but also verify the values of critical point and critical exponents.

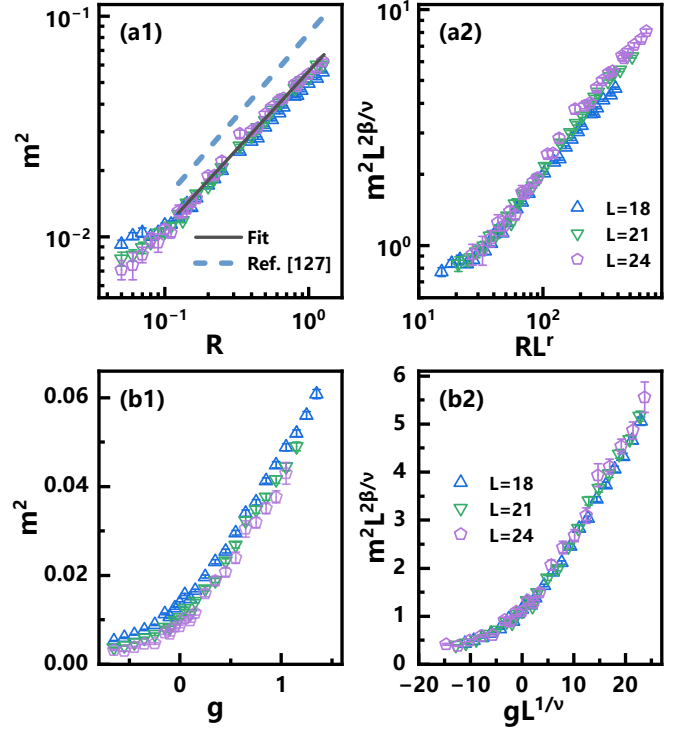


FIG. 3. Driven dynamics from the AFM phase of model (1). (a) Log-log plots of m^2 versus R for different L driven to $U_c = 3.85$ before (a1) and after (a2) rescaling. For large R , power fitting (black solid line) shows $m^2 \propto R^{0.71}$ with the exponent close to $2\beta/\nu r = 0.752$ (dash line) from Ref. [127]. (b) Curves of m^2 versus g for fixed $RL^r = 41.5$ and different L before (b1) and after (b2) rescaling.

In addition, to unravel the scaling properties in the whole driven process, we calculate the dependence of m^2 on g for an arbitrary fixed RL^r and present the results in Fig. 2 (b1). After rescaling m^2 and g by $L^{2\beta/\nu}$ and $L^{1/\nu}$ respectively, the curves with various L collapse into each other, as displayed in Fig. 2 (b2), confirming that the universal scaling behavior of physical observable in the whole driven process is described by Eq. (2).

The reason for the appearance of the scaling relation $m^2 \propto L^{-d} R^{(2\beta - d\nu)/\nu r}$ is that for large R , driven induced length scale $\xi_R \sim R^{-1/r}$ is smaller than L . Thus, the definition of m^2 indicates that $m^2 \propto L^{-d}$ owing to the central limit theorem. Meanwhile, the rest part of the dimension of m^2 should be borne by R , giving rise to the leading term of Eq. (2). In this case, $\mathcal{F}(x, 0)$ tends to a constant. In contrast, for small R , $\xi_R > L$ and the conventional finite-size scaling at equilibrium $m^2 \propto L^{-2\beta/\nu}$ is recovered, as confirmed in Fig. 2 (a2), and $\mathcal{F}(x, 0)$ obeys the scaling form $\mathcal{F}(x, 0) \sim x^{d/r - 2\beta/\nu r}$.

Next, we turn to explore the driven dynamics starting from the Mott insulator initial state. This state has the AFM order with transverse gapless modes. For large R , Fig. 3 (a1) shows that m^2 obeys $m^2 \propto R^{2\beta/\nu r}$ and is nearly independent of L . Combining this scaling relation

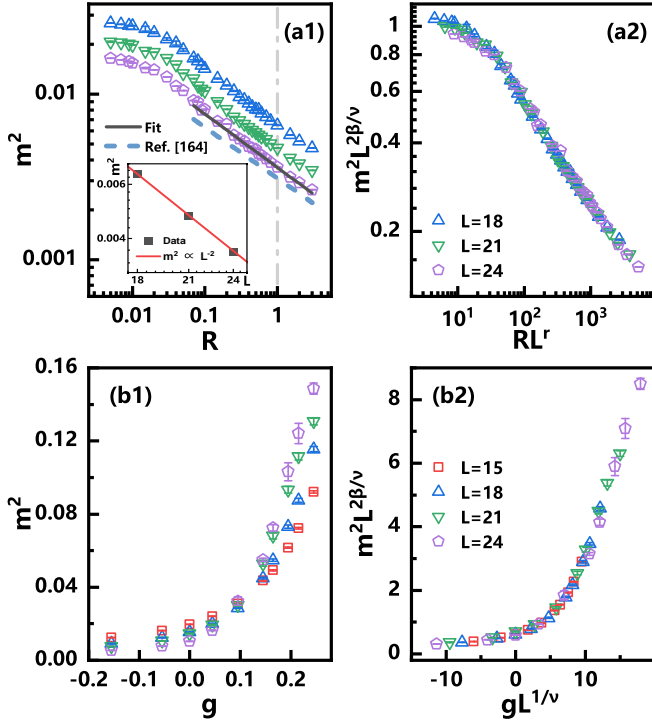


FIG. 4. Driven dynamics from the DSM phase of model (4). (a) Log-log plots of m^2 versus R for different L driven to $V_c = 1.355$ before (a1) and after (a2) rescaling. Inset in (a1) shows $m^2 \propto L^{-2}$ for $R = 1$ (dash-dotted line). For large R , power fitting for $L = 24$ (black solid line) shows $m^2 \propto R^{-0.32}$ with the exponent close to $(2\beta - d\nu)/\nu r = -0.31$ (dash line) from Ref. [164]. (b) Curves of m^2 versus g for fixed $RL^r = 63.34$ and different L before (b1) and after (b2) rescaling.

with the usual finite-size scaling $m^2 \propto L^{-2\beta/\nu}$ which is restored for small R , the scaling form should obey

$$m^2(R, L, g) = R^{2\beta/\nu r} \mathcal{G}(RL^r, gL^{1/\nu}), \quad (3)$$

where \mathcal{G} is the non-singular scaling function and g is also included therein. Eq. (3) is also accordant with the conventional FTS with ordered initial state [43–45]

We rescale curves of m^2 versus R for various L at $g = 0$ according to the scaling function $m^2(R, L, g) = L^{-2\beta/\nu} \mathcal{G}(RL^r, 0)$ and find that the rescaled curves collapse well, which confirms Eq. (3) at $g = 0$. Furthermore, Fig. 3 (b1) shows the curves of m^2 versus g for an arbitrary fixed RL^r . The rescaled results ($gL^{1/\nu}, m^2 L^{2\beta/\nu}$) for various L collapse into a single smooth curve, as displayed in Fig. 3 (b2), confirming that the driven process from AFM initial state is described by Eq. (3).

The appearance of $m^2 \propto R^{2\beta/\nu r}$ reflects the fact that when $\xi_R < L$ the initial ordered magnetization domain is maintained. In this case, $\mathcal{G}(x, 0)$ tends to a constant. In contrast, for small R with $\xi_R > L$, the usual finite size scaling is recovered, indicating $\mathcal{G}(x, 0) \sim x^{-2\beta/\nu r}$ as $x \rightarrow 0$.

Dynamics in chiral Ising criticality— To further verify the FTS in Dirac systems, we also explore the driven

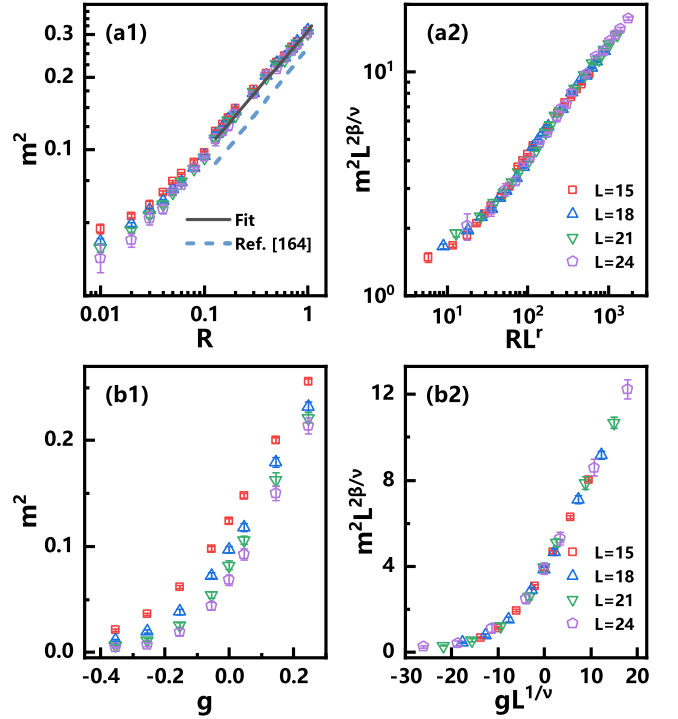


FIG. 5. Driven dynamics from the CDW phase of model (4). (a) Log-log plots of m^2 versus R for different L driven to $V_c = 1.355$ before (a1) and after (a2) rescaling. For large R , power fitting (black solid line) shows $m^2 \propto R^{0.50}$ with the exponent close to $2\beta/\nu r = 0.54$ from Ref. [164] (dash line). (b) Curves of m^2 versus g for fixed $RL^r = 87.97$ and different L before (b1) and after (b2) rescaling.

dynamics of Dirac QCP belonging to chiral Ising universality class, which is realized in the interacting spinless fermion model on the half-filled honeycomb lattice with the Hamiltonian [136, 137, 164–166]:

$$H = -t \sum_{\langle ij \rangle} c_i^\dagger c_j + V \sum_{\langle ij \rangle} \left(n_i - \frac{1}{2} \right) \left(n_j - \frac{1}{2} \right), \quad (4)$$

where V measures the nearest-neighbor interaction. The model is amenable to sign-problem-free QMC simulation [167–170]. It is shown that the ground state undergoes a continuous quantum phase transition at $V_c \approx 1.355t$ from the DSM phase to the charge-density-wave (CDW) insulating phase, characterized by the order parameter $m^2 \equiv \sum_{i,j} \eta_i \eta_j \langle (n_i - 1/2)(n_j - 1/2) \rangle / L^{2d}$ with $\eta_i = \pm 1$ for $i \in A(B)$ sublattice [136, 137, 164]. At $V = V_c$, both fermion and boson degrees of freedom are gapless, similar to model (1). However, a difference is that in the CDW phase, the bosonic fluctuation is fully gapped owing to the discrete symmetry breaking.

From the DSM initial state, Fig. 4 (a1) shows that fixed at $V = V_c$, namely $g = 0$, $m^2 \propto L^{-d} R^{(2\beta - d\nu)/\nu r}$ for large R , whereas $m^2 \propto L^{-2\beta/\nu}$ for small R , similar to the results in model (1). In addition, we find the rescaled curves of m^2 versus R and g collapse well, as shown in

Fig. 4 (a2) and (b2), confirming that Eq. (2) gives a universal description on the driven critical dynamics from the DSM initial state.

From the CDW initial state, Fig. 5 (a1) shows that at $g = 0$, $m^2 \propto R^{2\beta/\nu r}$ for large R , whereas $m^2 \propto L^{-2\beta/\nu}$ for small R , similar to the case of chiral Heisenberg universality class. Moreover, Eq. (3) is verified by the data collapse of the curves ($RL^r, m^2 L^{-2\beta/\nu}$) at fixed $g = 0$ and ($gL^{1/\nu}, m^2 L^{-2\beta/\nu}$) for an arbitrary RL^r , as shown in Fig. 5 (a2) and (b2). Consequently, Eq. (3) provides a universal description on the driven dynamics from ordered initial states, regardless of whether or not gapless bosonic modes exist.

Discussion— Some remarks are discussed as follows.

(a) A crucial prerequisite in the original KZM is the existence of initial adiabatic stage in which the excitations possess finite gap [1, 2, 163]. In contrast, the FTS of driven critical dynamics still holds in Dirac systems, indicating that this requirement is not indispensable, since in both quantum phases separated by the QCP the gapless excitations are present: the DSM phase features gapless fermions, whereas bosonic gapless excitation exists in the AFM Mott insulator phase where continuous symmetry is spontaneously broken.

To understand the underlying reasons of the novel numerical results, we notice that the DSM phase has the vanishing density of states at charge neutral point. Moreover, the Pauli principle of fermions further restricts the excitations in the vicinity of Dirac points. Accordingly, the excitations under slow external driving are strongly suppressed in DSM phase. Hence, it is speculated that the theories of KZM and FTS in driven dynamics are generally obeyed in Dirac QCP with the initial state of DSM. Besides, for driven dynamics from the AFM initial state, since we focus on the dynamic scaling of the order parameter magnitude, the influence of gapless angular excitation is tiny since its characteristic time scale is much longer than that of longitudinal mode [171], similar to the case in deconfined quantum criticality [51].

(b) Furthermore, our work provides an effective approach to assess fermionic critical properties from the perspective of nonequilibrium driven dynamics. Large discrepancy on critical exponents of chiral Heisenberg universality class still exists even under extensive studies [126, 127]. Here, by means of FTS analysis we reveal that the critical exponents for large R in Figs. 2 and 3 are consistent with the ones from Ref. [127], in which results of larger system size and careful finite-size corrections are included. For the finite-size scaling of equilibrium QCP, the critical exponents are extracted by the scaling analysis with varying interaction strength and system size. In the framework of driven dynamics, the driven rate R constitutes a new tuning parameter, enabling the achievement of critical exponents with fixing $g = 0$ or $L = L_{\max}$ according to Eqs. (2) and (3), which offers a possible way to mitigating sub-leading corrections arising from finite

g or small system size. Consequently, the reliable values of critical exponents are accessible with relatively small system size.

Summary— In summary, we investigate the driven dynamics of QCP in two representative interacting Dirac-fermion systems, belonging to chiral Heisenberg and chiral Ising universality classes respectively, through sign-problem-free QMC simulation. Driving the system from both DSM and Mott insulator phase as the initial state, we discover varieties of interesting nonequilibrium scaling behaviors. Furthermore, we confirm that these scaling behaviors can be unified by the full scaling form of the FTS theory. Through this work we not only successfully generalize the KZM and FTS to critical systems with joint fluctuations of gapless fermions and bosons, but also extend the application conditions of the celebrated theory of KZM. Additionally, we demonstrate that the nonequilibrium scaling form is capable of determining the critical exponents in Dirac QCP, providing an effective method to deciphering quantum critical properties in terms of driven dynamics. Our work possesses many intriguing generalizations, for example, it is quite instructive to consider other kinds of driven protocols, such as driving from the critical point and from the thermal equilibrium state [38–40, 172, 173]. From the experimental perspectives, the Moiré systems of graphene and heterostructures offer tunable platforms to observe the fermionic QCP and the associated driven critical dynamics [174, 175]. Moreover, as aforementioned, the Kibble-Zurek driven dynamics is experimentally observed in cold-atom systems [30, 41]. Owing to the recent developments of cold atoms based quantum simulator of fermions [176–178], it is promising to detect driven dynamics in Dirac QCP and verify the generalized KZM and FTS as discussed in our study in these platforms.

Acknowledgments— We would like to thank A. W. Sandvik for helpful discussions. Z. Zeng, Y. K. Yu, Z. X. Li and S. Yin are supported by the National Natural Science Foundation of China (Grants No. 12075324 and No. 12222515). Z. X. Li is supported by the NSFC under Grant No. 12347107. S. Yin is also supported by the Science and Technology Projects in Guangdong Province (Grants No. 211193863020). The calculations reported were partly performed on resources provided by the Guangdong Provincial Key Laboratory of Magnetoelectric Physics and Devices, No. 2022B1212010008.

* These authors contribute equally to this work.

† zixiangli@iphy.ac.cn

‡ yinsh6@mail.sysu.edu.cn

- [1] J. Dziarmaga, *Advances in Physics* **59**, 1063 (2010).
- [2] A. Polkovnikov, K. Sengupta, A. Silva, and M. Venugattore, *Rev. Mod. Phys.* **83**, 863 (2011).
- [3] L. D'Alessio, Y. Kafri, A. Polkovnikov, and M. Rigol,

- Advances in Physics* **65**, 239 (2016).
- [4] A. Mitra, *Annual Review of Condensed Matter Physics* **9**, 245 (2018).
 - [5] T. W. B. Kibble, *Journal of Physics A: Mathematical and General* **9**, 1387 (1976).
 - [6] W. H. Zurek, *Nature* **317**, 505 (1985).
 - [7] P. Laguna and W. H. Zurek, *Phys. Rev. Lett.* **78**, 2519 (1997).
 - [8] M. Hindmarsh and A. Rajantie, *Phys. Rev. Lett.* **85**, 4660 (2000).
 - [9] I. Chuang, R. Durrer, N. Turok, and B. Yurke, *Science* **251**, 1336 (1991), <https://www.science.org/doi/pdf/10.1126/science.251.4999.1336>.
 - [10] J. Dziarmaga, *Phys. Rev. Lett.* **81**, 5485 (1998).
 - [11] W. H. Zurek, U. Dorner, and P. Zoller, *Phys. Rev. Lett.* **95**, 105701 (2005).
 - [12] J. Dziarmaga, *Phys. Rev. Lett.* **95**, 245701 (2005).
 - [13] B. Damski and W. H. Zurek, *Phys. Rev. Lett.* **99**, 130402 (2007).
 - [14] G. Lamporesi, S. Donadello, S. Serafini, F. Dalfovo, and G. Ferrari, *Nature Physics* **9**, 656 (2013).
 - [15] N. Navon, A. L. Gaunt, R. P. Smith, and Z. Hadzibabic, *Science* **347**, 167 (2015), <https://www.science.org/doi/pdf/10.1126/science.1258676>.
 - [16] K. Du, X. Fang, C. Won, C. De, F.-T. Huang, W. Xu, H. You, F. J. Gómez-Ruiz, A. del Campo, and S.-W. Cheong, *Nature Physics* **19**, 1495 (2023).
 - [17] B. Ko, J. W. Park, and Y. Shin, *Nature Physics* **15**, 1227 (2019).
 - [18] L. Ulčakar, J. Mravlje, and T. c. v. Rejec, *Phys. Rev. Lett.* **125**, 216601 (2020).
 - [19] P. J. D. Crowley, I. Martin, and A. Chandran, *Phys. Rev. Lett.* **125**, 100601 (2020).
 - [20] F. J. Gómez-Ruiz, J. J. Mayo, and A. del Campo, *Phys. Rev. Lett.* **124**, 240602 (2020).
 - [21] J. Goo, Y. Lim, and Y. Shin, *Phys. Rev. Lett.* **127**, 115701 (2021).
 - [22] S. Maegochi, K. Ienaga, and S. Okuma, *Phys. Rev. Lett.* **129**, 227001 (2022).
 - [23] J. Dziarmaga, M. M. Rams, and W. H. Zurek, *Phys. Rev. Lett.* **129**, 260407 (2022).
 - [24] N. E. Sherman, A. Avdoshkin, and J. E. Moore, *Phys. Rev. Lett.* **131**, 106501 (2023).
 - [25] F. Balducci, M. Beau, J. Yang, A. Gambassi, and A. del Campo, *Phys. Rev. Lett.* **131**, 230401 (2023).
 - [26] H.-B. Zeng, C.-Y. Xia, and A. del Campo, *Phys. Rev. Lett.* **130**, 060402 (2023).
 - [27] G. Lamporesi, S. Donadello, S. Serafini, F. Dalfovo, and G. Ferrari, *Nature Physics* **9**, 656 (2013).
 - [28] R. Barends, A. Shabani, L. Lamata, J. Kelly, A. Mezzacapo, U. L. Heras, R. Babbush, A. G. Fowler, B. Campbell, Y. Chen, Z. Chen, B. Chiaro, A. Dunsworth, E. Jeffrey, E. Lucero, A. Megrant, J. Y. Mutus, M. Neeley, C. Neill, P. J. J. O'Malley, C. Quintana, P. Roushan, D. Sank, A. Vainsencher, J. Wenner, T. C. White, E. Solano, H. Neven, and J. M. Martinis, *Nature* **534**, 222 (2016).
 - [29] A. D. King, S. Suzuki, J. Raymond, A. Zucca, T. Lanting, F. Altomare, A. J. Berkley, S. Ejtemaee, E. Hoskinson, S. Huang, E. Ladizinsky, A. J. R. MacDonald, G. Marsden, T. Oh, G. Poulin-Lamarre, M. Reis, C. Rich, Y. Sato, J. D. Whittaker, J. Yao, R. Harris, D. A. Lidar, H. Nishimori, and M. H. Amin, *Nature Physics* **18**, 1324 (2022).
 - [30] A. Keesling, A. Omran, H. Levine, H. Bernien, H. Pichler, S. Choi, R. Samajdar, S. Schwartz, P. Silvi, S. Sachdev, P. Zoller, M. Endres, M. Greiner, V. Vuletić, and M. D. Lukin, *Nature* **568**, 207 (2019).
 - [31] S. Ebadi, T. T. Wang, H. Levine, A. Keesling, G. Semeghini, A. Omran, D. Bluvstein, R. Samajdar, H. Pichler, W. W. Ho, S. Choi, S. Sachdev, M. Greiner, V. Vuletić, and M. D. Lukin, *Nature* **595**, 227 (2021).
 - [32] K.-X. Yao, Z. Zhang, and C. Chin, *Nature* **602**, 68 (2022).
 - [33] L.-Y. Qiu, H.-Y. Liang, Y.-B. Yang, H.-X. Yang, T. Tian, Y. Xu, and L.-M. Duan, *Science Advances* **6**, eaba7292 (2020), <https://www.science.org/doi/pdf/10.1126/sciadv.aba7292>.
 - [34] S. Ebadi, A. Keesling, M. Cain, T. T. Wang, H. Levine, D. Bluvstein, G. Semeghini, A. Omran, J.-G. Liu, R. Samajdar, X.-Z. Luo, B. Nash, X. Gao, B. Barak, E. Farhi, S. Sachdev, N. Gemelke, L. Zhou, S. Choi, H. Pichler, S.-T. Wang, M. Greiner, V. Vuletić, and M. D. Lukin, *Science* **376**, 1209 (2022), <https://www.science.org/doi/pdf/10.1126/science.abo6587>.
 - [35] S. Sunami, V. P. Singh, D. Garrick, A. Beregi, A. J. Barker, K. Luksch, E. Bentine, L. Mathey, and C. J. Foot, *Science* **382**, 443 (2023), <https://www.science.org/doi/pdf/10.1126/science.abq6753>.
 - [36] B.-W. Li, Y.-K. Wu, Q.-X. Mei, R. Yao, W.-Q. Lian, M.-L. Cai, Y. Wang, B.-X. Qi, L. Yao, L. He, Z.-C. Zhou, and L.-M. Duan, *PRX Quantum* **4**, 010302 (2023).
 - [37] F. Zhong and Z. Xu, *Phys. Rev. B* **71**, 132402 (2005).
 - [38] S. Deng, G. Ortiz, and L. Viola, *Europhysics Letters* **84**, 67008 (2009).
 - [39] C. De Grandi, V. Gritsev, and A. Polkovnikov, *Phys. Rev. B* **81**, 012303 (2010).
 - [40] A. Chandran, A. Erez, S. S. Gubser, and S. L. Sondhi, *Phys. Rev. B* **86**, 064304 (2012).
 - [41] L. W. Clark, L. Feng, and C. Chin, *Science* **354**, 606 (2016), <https://www.science.org/doi/pdf/10.1126/science.aaf9657>.
 - [42] M. Kolodrubetz, B. K. Clark, and D. A. Huse, *Phys. Rev. Lett.* **109**, 015701 (2012).
 - [43] S. Gong, F. Zhong, X. Huang, and S. Fan, *New Journal of Physics* **12**, 043036 (2010).
 - [44] B. Feng, S. Yin, and F. Zhong, *Phys. Rev. B* **94**, 144103 (2016).
 - [45] Y. Huang, S. Yin, B. Feng, and F. Zhong, *Phys. Rev. B* **90**, 134108 (2014).
 - [46] C.-W. Liu, A. Polkovnikov, and A. W. Sandvik, *Phys. Rev. B* **89**, 054307 (2014).
 - [47] S. Yin, P. Mai, and F. Zhong, *Phys. Rev. B* **89**, 094108 (2014).
 - [48] C.-W. Liu, A. Polkovnikov, and A. W. Sandvik, *Phys. Rev. Lett.* **114**, 147203 (2015).
 - [49] S. Yin, G.-Y. Huang, C.-Y. Lo, and P. Chen, *Phys. Rev. Lett.* **118**, 065701 (2017).
 - [50] Y. Li, Z. Zeng, and F. Zhong, *Phys. Rev. E* **100**, 020105 (2019).
 - [51] Y.-R. Shu, S.-K. Jian, A. W. Sandvik, and S. Yin, *arXiv: 2305.04771* (2023).
 - [52] A. D. King, J. Raymond, T. Lanting, R. Harris, A. Zucca, F. Altomare, A. J. Berkley, K. Boothby, S. Ejtemaee, C. Enderud, E. Hoskinson, S. Huang, E. Ladizinsky, A. J. R. MacDonald, G. Marsden, R. Molavi, T. Oh, G. Poulin-Lamarre, M. Reis, C. Rich, Y. Sato, N. Tsai, M. Volkmann, J. D. Whittaker, J. Yao,

- A. W. Sandvik, and M. H. Amin, *Nature* **617**, 61 (2023).
- [53] J. S. Garcia and N. Chepiga, “Resolving chiral transitions in rydberg arrays with quantum kibble-zurek mechanism and finite-time scaling,” (2024), [arXiv:2403.03081](https://arxiv.org/abs/2403.03081) [cond-mat.str-el].
- [54] A. D. King, A. Nocera, M. M. Rams, J. Dziarmaga, R. Wiersema, W. Bernoudy, J. Raymond, N. Kaushal, N. Heinsdorf, R. Harris, K. Boothby, F. Altomare, A. J. Berkley, M. Boschnak, K. Chern, H. Christiani, S. Cibere, J. Connor, M. H. Dehn, R. Deshpande, S. Ejtemaee, P. Farré, K. Hamer, E. Hoskinson, S. Huang, M. W. Johnson, S. Kortas, E. Ladizinsky, T. Lai, T. Lanting, R. Li, A. J. R. MacDonald, G. Marsden, C. C. McGeoch, R. Molavi, R. Neufeld, M. Norouzpour, T. Oh, J. Pasvolsky, P. Poitras, G. Poulin-Lamarre, T. Prescott, M. Reis, C. Rich, M. Samani, B. Sheldan, A. Smirnov, E. Sterpka, B. T. Clavera, N. Tsai, M. Volkmann, A. Whitticar, J. D. Whittaker, W. Wilkinson, J. Yao, T. J. Yi, A. W. Sandvik, G. Alvarez, R. G. Melko, J. Carrasquilla, M. Franz, and M. H. Amin, “Computational supremacy in quantum simulation,” (2024), [arXiv:2403.00910](https://arxiv.org/abs/2403.00910) [quant-ph].
- [55] M. Dupont and J. E. Moore, *Phys. Rev. B* **106**, L041109 (2022).
- [56] S. Sachdev, *Quantum Phase Transitions*, 2nd ed. (Cambridge Univ. Press, 2011).
- [57] J. A. Hertz, *Phys. Rev. B* **14**, 1165 (1976).
- [58] A. J. Millis, *Phys. Rev. B* **48**, 7183 (1993).
- [59] E. Berg, S. Lederer, Y. Schattner, and S. Trebst, *Annual Review of Condensed Matter Physics* **10**, 63 (2019), <https://doi.org/10.1146/annurev-conmatphys-031218-013339>.
- [60] H. v. Löhneysen, A. Rosch, M. Vojta, and P. Wölfle, *Rev. Mod. Phys.* **79**, 1015 (2007).
- [61] S.-S. Lee, *Annual Review of Condensed Matter Physics* **9**, 227 (2018), <https://doi.org/10.1146/annurev-conmatphys-031016-025531>.
- [62] M. A. Metlitski and S. Sachdev, *Phys. Rev. B* **82**, 075127 (2010).
- [63] H. Yezhakov and J. Maciejko, *Phys. Rev. B* **98**, 195142 (2018).
- [64] I. Esterlis, H. Guo, A. A. Patel, and S. Sachdev, *Phys. Rev. B* **103**, 235129 (2021).
- [65] A. V. Chubukov, C. Pépin, and J. Rech, *Phys. Rev. Lett.* **92**, 147003 (2004).
- [66] S. Paschen and Q. Si, *Nature Reviews Physics* **3**, 9 (2021).
- [67] G. R. Stewart, *Rev. Mod. Phys.* **56**, 755 (1984).
- [68] Q. Si, S. Rabello, K. Ingersent, and J. L. Smith, *Nature* **413**, 804 (2001).
- [69] J. Custers, P. Gegenwart, H. Wilhelm, K. Neumaier, Y. Tokiwa, O. Trovarelli, C. Geibel, F. Steglich, C. Pépin, and P. Coleman, *Nature* **424**, 524 (2003).
- [70] T. Senthil, M. Vojta, and S. Sachdev, *Phys. Rev. B* **69**, 035111 (2004).
- [71] B. Keimer, S. A. Kivelson, M. R. Norman, S. Uchida, and J. Zaanen, *Nature* **518**, 179 (2015).
- [72] P. A. Lee, N. Nagaosa, and X.-G. Wen, *Rev. Mod. Phys.* **78**, 17 (2006).
- [73] S. Sachdev, *Rev. Mod. Phys.* **75**, 913 (2003).
- [74] X. Chen, P. Dai, D. Feng, T. Xiang, and F.-C. Zhang, *National Science Review* **1**, 371 (2014).
- [75] D.-H. Lee, *Annual Review of Condensed Matter Physics* **9**, 261 (2018).
- [76] R. M. Fernandes, A. I. Coldea, H. Ding, I. R. Fisher, P. J. Hirschfeld, and G. Kotliar, *Nature* **601**, 35 (2022).
- [77] Y. Cao, V. Fatemi, A. Demir, S. Fang, S. L. Tomarken, J. Y. Luo, J. D. Sanchez-Yamagishi, K. Watanabe, T. Taniguchi, E. Kaxiras, R. C. Ashoori, and P. Jarillo-Herrero, *Nature* **556**, 80 (2018).
- [78] Y. Cao, V. Fatemi, S. Fang, K. Watanabe, T. Taniguchi, E. Kaxiras, and P. Jarillo-Herrero, *Nature* **556**, 43 (2018).
- [79] A. Jaoui, I. Das, G. Di Battista, J. Díez-Mérida, X. Lu, K. Watanabe, T. Taniguchi, H. Ishizuka, L. Levitov, and D. K. Efetov, *Nature Physics* **18**, 633 (2022).
- [80] E. Y. Andrei and A. H. MacDonald, *Nature Materials* **19**, 1265 (2020).
- [81] L. Prochaska, X. Li, D. C. MacFarland, A. M. Andrews, M. Bonta, E. F. Bianco, S. Yazdi, W. Schrenk, H. Detz, A. Limbeck, Q. Si, E. Ringe, G. Strasser, J. Kono, and S. Paschen, *Science* **367**, 285 (2020), <https://www.science.org/doi/pdf/10.1126/science.aag1595>.
- [82] A. A. Patel, H. Guo, I. Esterlis, and S. Sachdev, *Science* **381**, 790 (2023), <https://www.science.org/doi/pdf/10.1126/science.abq6011>.
- [83] B. Shen, Y. Zhang, Y. Komijani, M. Nicklas, R. Borth, A. Wang, Y. Chen, Z. Nie, R. Li, X. Lu, H. Lee, M. Smidman, F. Steglich, P. Coleman, and H. Yuan, *Nature* **579**, 51 (2020).
- [84] C. M. Varma, *Rev. Mod. Phys.* **92**, 031001 (2020).
- [85] P. W. Phillips, N. E. Hussey, and P. Abbamonte, *Science* **377**, eab4273 (2022), <https://www.science.org/doi/pdf/10.1126/science.abh4273>.
- [86] D. J. Scalapino, *Rev. Mod. Phys.* **84**, 1383 (2012).
- [87] S. Lederer, Y. Schattner, E. Berg, and S. A. Kivelson, *Phys. Rev. Lett.* **114**, 097001 (2015).
- [88] Z.-X. Li, F. Wang, H. Yao, and D.-H. Lee, *Science Bulletin* **61**, 925 (2016).
- [89] E. Berg, M. A. Metlitski, and S. Sachdev, *Science* **338**, 1606 (2012).
- [90] D. v. d. Marel, H. J. A. Molegraaf, J. Zaanen, Z. Nussinov, F. Carbone, A. Damascelli, H. Eisaki, M. Greven, P. H. Kes, and M. Li, *Nature* **425**, 271 (2003).
- [91] S. A. Kivelson, I. P. Bindloss, E. Fradkin, V. Oganesyan, J. M. Tranquada, A. Kapitulnik, and C. Howald, *Rev. Mod. Phys.* **75**, 1201 (2003).
- [92] E. Fradkin, S. A. Kivelson, and J. M. Tranquada, *Rev. Mod. Phys.* **87**, 457 (2015).
- [93] Y. Schattner, S. Lederer, S. A. Kivelson, and E. Berg, *Phys. Rev. X* **6**, 031028 (2016).
- [94] X. Wang, Y. Wang, Y. Schattner, E. Berg, and R. M. Fernandes, *Phys. Rev. Lett.* **120**, 247002 (2018).
- [95] Z.-X. Li, F. Wang, H. Yao, and D.-H. Lee, *Phys. Rev. B* **95**, 214505 (2017).
- [96] M. H. Gerlach, Y. Schattner, E. Berg, and S. Trebst, *Phys. Rev. B* **95**, 035124 (2017).
- [97] C. M. Varma, *Phys. Rev. Lett.* **83**, 3538 (1999).
- [98] D. J. Gross and A. Neveu, *Phys. Rev. D* **10**, 3235 (1974).
- [99] B. Roy, V. Juričić, and I. F. Herbut, *Journal of High Energy Physics* **2016**, 18 (2016).
- [100] J. A. Gracey, T. Luthe, and Y. Schröder, *Phys. Rev. D* **94**, 125028 (2016).
- [101] F. Gehring, H. Gies, and L. Janssen, *Phys. Rev. D* **92**, 085046 (2015).
- [102] D. Poland, S. Rychkov, and A. Vichi, *Rev. Mod. Phys.* **91**, 015002 (2019).

- [103] S. Gazit, M. Randeria, and A. Vishwanath, *Nature Physics* **13**, 484 (2017).
- [104] Y.-Z. You, Y.-C. He, C. Xu, and A. Vishwanath, *Phys. Rev. X* **8**, 011026 (2018).
- [105] K. Ladovrechis, S. Ray, T. Meng, and L. Janssen, *Phys. Rev. B* **107**, 035151 (2023).
- [106] L. Janssen and I. F. Herbut, *Phys. Rev. B* **89**, 205403 (2014).
- [107] F. Parisen Toldin, M. Hohenadler, F. F. Assaad, and I. F. Herbut, *Phys. Rev. B* **91**, 165108 (2015).
- [108] B. Knorr, *Phys. Rev. B* **94**, 245102 (2016).
- [109] B. Ihrig, L. N. Mihaila, and M. M. Scherer, *Phys. Rev. B* **98**, 125109 (2018).
- [110] R. Boyack, H. Yezhakov, and J. Maciejko, *The European Physical Journal Special Topics* **230**, 979 (2021).
- [111] T. C. Lang and A. M. Läuchli, *Phys. Rev. Lett.* **123**, 137602 (2019).
- [112] Z. H. Liu, W. Jiang, B.-B. Chen, J. Rong, M. Cheng, K. Sun, Z. Y. Meng, and F. F. Assaad, *Phys. Rev. Lett.* **130**, 266501 (2023).
- [113] Z.-X. Li, A. Vaezi, C. B. Mendl, and H. Yao, *Science Advances* **4**, eaau1463 (2018).
- [114] Z. Zhou, D. Wang, Z. Y. Meng, Y. Wang, and C. Wu, *Phys. Rev. B* **93**, 245157 (2016).
- [115] S. M. Tabatabaei, A.-R. Negari, J. Maciejko, and A. Vaezi, *Phys. Rev. Lett.* **128**, 225701 (2022).
- [116] Y. Otsuka, K. Seki, S. Sorella, and S. Yunoki, *Phys. Rev. B* **98**, 035126 (2018).
- [117] X. Y. Xu and T. Grover, *Phys. Rev. Lett.* **126**, 217002 (2021).
- [118] S. Chandrasekharan and A. Li, *Phys. Rev. D* **88**, 021701 (2013).
- [119] T.-T. Wang and Z. Y. Meng, “Emus live on the gossneveu-yukawa archipelago,” (2023), [arXiv:2304.00034](https://arxiv.org/abs/2304.00034) [cond-mat.str-el].
- [120] X.-J. Yu, Z. Pan, L. Xu, and Z.-X. Li, *Phys. Rev. Lett.* **132**, 116503 (2024).
- [121] H. Xu, X. Li, Z. Zhou, X. Wang, L. Wang, C. Wu, and Y. Wang, *Phys. Rev. Res.* **5**, 023180 (2023).
- [122] X. Zhu, Y. Huang, H. Guo, and S. Feng, *Phys. Rev. B* **106**, 075109 (2022).
- [123] S. Sorella and E. Tosatti, *Europhysics Letters* **19**, 699 (1992).
- [124] I. F. Herbut, *Phys. Rev. Lett.* **97**, 146401 (2006).
- [125] I. F. Herbut, V. Juričić, and O. Vafek, *Phys. Rev. B* **80**, 075432 (2009).
- [126] F. F. Assaad and I. F. Herbut, *Phys. Rev. X* **3**, 031010 (2013).
- [127] Y. Otsuka, S. Yunoki, and S. Sorella, *Phys. Rev. X* **6**, 011029 (2016).
- [128] L. N. Mihaila, N. Zerf, B. Ihrig, I. F. Herbut, and M. M. Scherer, *Phys. Rev. B* **96**, 165133 (2017).
- [129] N. Zerf, L. N. Mihaila, P. Marquard, I. F. Herbut, and M. M. Scherer, *Phys. Rev. D* **96**, 096010 (2017).
- [130] T. Grover, D. N. Sheng, and A. Vishwanath, *Science* **344**, 280 (2014).
- [131] U. F. P. Seifert, X.-Y. Dong, S. Chulliparambil, M. Vojta, H.-H. Tu, and L. Janssen, *Phys. Rev. Lett.* **125**, 257202 (2020).
- [132] S. Ray and L. Janssen, *Phys. Rev. B* **104**, 045101 (2021).
- [133] P. Corboz, P. Czarnik, G. Kapteijns, and L. Tagliacozzo, *Phys. Rev. X* **8**, 031031 (2018).
- [134] M. Rader and A. M. Läuchli, *Phys. Rev. X* **8**, 031030 (2018).
- [135] Y. Da Liao, X. Y. Xu, Z. Y. Meng, and Y. Qi, *Phys. Rev. B* **106**, 075111 (2022).
- [136] L. Wang, P. Corboz, and M. Troyer, *New Journal of Physics* **16**, 103008 (2014).
- [137] Z.-X. Li, Y.-F. Jiang, and H. Yao, *New Journal of Physics* **17**, 085003 (2015).
- [138] Y. Liu, Z. Wang, T. Sato, W. Guo, and F. F. Assaad, *Phys. Rev. B* **104**, 035107 (2021).
- [139] Z. H. Liu, M. Vojta, F. F. Assaad, and L. Janssen, *Phys. Rev. Lett.* **128**, 087201 (2022).
- [140] C. Chen, X. Y. Xu, Z. Y. Meng, and M. Hohenadler, *Phys. Rev. Lett.* **122**, 077601 (2019).
- [141] Y.-X. Zhang, W.-T. Chiu, N. C. Costa, G. G. Batrouni, and R. T. Scalettar, *Phys. Rev. Lett.* **122**, 077602 (2019).
- [142] B. Roy and S. Das Sarma, *Phys. Rev. B* **94**, 115137 (2016).
- [143] S. Han, G. Y. Cho, and E.-G. Moon, *Phys. Rev. B* **98**, 085149 (2018).
- [144] I. F. Herbut, “Wilson-fisher fixed points in presence of dirac fermions,” (2023), [arXiv:2304.07654](https://arxiv.org/abs/2304.07654) [cond-mat.str-el].
- [145] Y. Otsuka, K. Seki, S. Sorella, and S. Yunoki, *Phys. Rev. B* **102**, 235105 (2020).
- [146] Z.-X. Li, Y.-F. Jiang, S.-K. Jian, and H. Yao, *Nature Communications* **8**, 314 (2017).
- [147] B.-H. Li, Z.-X. Li, and H. Yao, *Phys. Rev. B* **101**, 085105 (2020).
- [148] E. Torres, L. Classen, I. F. Herbut, and M. M. Scherer, *Phys. Rev. B* **97**, 125137 (2018).
- [149] L. Classen, I. F. Herbut, and M. M. Scherer, *Phys. Rev. B* **96**, 115132 (2017).
- [150] S. Yin and Z.-Y. Zuo, *Phys. Rev. B* **101**, 155136 (2020).
- [151] A. H. Castro Neto, F. Guinea, N. M. R. Peres, K. S. Novoselov, and A. K. Geim, *Rev. Mod. Phys.* **81**, 109 (2009).
- [152] M. Z. Hasan and C. L. Kane, *Rev. Mod. Phys.* **82**, 3045 (2010).
- [153] X.-L. Qi and S.-C. Zhang, *Rev. Mod. Phys.* **83**, 1057 (2011).
- [154] F. Assaad and H. Evertz, “World-line and determinantal quantum monte carlo methods for spins, phonons and electrons,” in *Computational Many-Particle Physics*, edited by H. Fehske, R. Schneider, and A. Weiße (Springer Berlin Heidelberg, Berlin, Heidelberg, 2008) pp. 277–356.
- [155] M. Troyer and U.-J. Wiese, *Phys. Rev. Lett.* **94**, 170201 (2005).
- [156] Z.-X. Li and H. Yao, *Annual Review of Condensed Matter Physics* **10**, 337 (2019), <https://doi.org/10.1146/annurev-conmatphys-033117-054307>.
- [157] M. Schmitt, M. M. Rams, J. Dziarmaga, M. Heyl, and W. H. Zurek, *Science Advances* **8**, eabl6850 (2022), <https://www.science.org/doi/pdf/10.1126/sciadv.abl6850>.
- [158] J. Dziarmaga and J. M. Mazur, *Phys. Rev. B* **107**, 144510 (2023).
- [159] C. De Grandi, A. Polkovnikov, and A. W. Sandvik, *Phys. Rev. B* **84**, 224303 (2011).
- [160] C. D. Grandi, A. Polkovnikov, and A. W. Sandvik, *Journal of Physics: Condensed Matter* **25**, 404216 (2013).
- [161] C.-W. Liu, A. Polkovnikov, and A. W. Sandvik, *Phys. Rev. B* **87**, 174302 (2013).

- [162] C. Wu and S.-C. Zhang, *Phys. Rev. B* **71**, 155115 (2005).
- [163] A. Polkovnikov and V. Gritsev, *Nature Physics* **4**, 477 (2008).
- [164] S. Hesselmann and S. Wessel, *Phys. Rev. B* **93**, 155157 (2016).
- [165] L. Wang, Y.-H. Liu, and M. Troyer, *Phys. Rev. B* **93**, 155117 (2016).
- [166] S. Hesselmann, D. D. Scherer, M. M. Scherer, and S. Wessel, *Phys. Rev. B* **98**, 045142 (2018).
- [167] Z.-X. Li, Y.-F. Jiang, and H. Yao, *Phys. Rev. B* **91**, 241117 (2015).
- [168] Z.-X. Li, Y.-F. Jiang, and H. Yao, *Phys. Rev. Lett.* **117**, 267002 (2016).
- [169] Z. C. Wei, C. Wu, Y. Li, S. Zhang, and T. Xiang, *Phys. Rev. Lett.* **116**, 250601 (2016).
- [170] L. Wang, Y.-H. Liu, M. Iazzi, M. Troyer, and G. Harcos, *Physical review letters* **115**, 250601 (2015).
- [171] P. Weinberg and A. W. Sandvik, *Phys. Rev. B* **96**, 054442 (2017).
- [172] Y. Huang, S. Yin, Q. Hu, and F. Zhong, *Phys. Rev. B* **93**, 024103 (2016).
- [173] S. Yin, C.-Y. Lo, and P. Chen, *Phys. Rev. B* **94**, 064302 (2016).
- [174] D. M. Kennes, M. Claassen, L. Xian, A. Georges, A. J. Millis, J. Hone, C. R. Dean, D. N. Basov, A. N. Pasupathy, and A. Rubio, *Nature Physics* **17**, 155 (2021).
- [175] Q. Li, B. Cheng, M. Chen, B. Xie, Y. Xie, P. Wang, F. Chen, Z. Liu, K. Watanabe, T. Taniguchi, S.-J. Liang, D. Wang, C. Wang, Q.-H. Wang, J. Liu, and F. Miao, *Nature* **609**, 479 (2022).
- [176] R. Jördens, N. Strohmaier, K. Günter, H. Moritz, and T. Esslinger, *Nature* **455**, 204 (2008).
- [177] A. Mazurenko, C. S. Chiu, G. Ji, M. F. Parsons, M. Kanász-Nagy, R. Schmidt, F. Grusdt, E. Demler, D. Greif, and M. Greiner, *Nature* **545**, 462 (2017).
- [178] V. Venu, P. Xu, M. Mamaev, F. Corapi, T. Bilitewski, J. P. D’Incao, C. J. Fujiwara, A. M. Rey, and J. H. Thywissen, *Nature* **613**, 262 (2023).
- [179] R. K. Kaul, *Phys. Rev. Lett.* **115**, 157202 (2015).

Supplementary Materials for

Finite-time Scaling beyond the Kibble-Zurek Prerequisite: Driven Critical Dynamics in Strongly Interacting Dirac Systems

IMAGINARY-TIME DRIVEN DYNAMICS

The driven dynamics is realized by varying U with imaginary time τ as $U = U_0 + R\tau$, starting from the ground state at U_0 . The wave function $|\psi(\tau)\rangle$ obeys the imaginary-time Schrödinger equation [159–161]

$$-\frac{\partial}{\partial\tau}|\psi(\tau)\rangle = H(\tau)|\psi(\tau)\rangle. \quad (\text{S1})$$

The formal solution of Eq. (S1) is given by $|\psi(\tau)\rangle = U(\tau, 0)|\psi(0)\rangle$ in which $U(\tau, 0) = T_\tau \exp[-\int_0^\tau d\tau' H(\tau')]$ with T_τ being the time-ordering operator in imaginary-time direction. Since the model (1) and (4) is sign-problem-free and imaginary-time evolution does not induce additional sign problem, the imaginary-time dynamics of the model can be simulated by the large-scale determinant QMC method.

DETERMINANT QUANTUM MONTE CARLO

We employ the large-scale determinant QMC method [154] to investigate the imaginary-time driven dynamics of our models. Specifically, we start with a trial wave function $|\psi_T\rangle$, and project the system onto the desired initial state $|\psi_0\rangle$ with a sufficiently long projection time τ_0 . Then we vary the system parameter linearly with imaginary time variable τ and observe the scaling behavior of observables at final state, at which the expectation value of observables is given by

$$\langle O(\tau) \rangle = \frac{\langle \psi_0 | U(2\tau, \tau) O U(\tau, 0) | \psi_0 \rangle}{\langle \psi_0 | U(2\tau, 0) | \psi_0 \rangle} = \frac{\langle \psi_T | e^{-\tau_0 H_{\text{initial}}} U(2\tau, \tau) O U(\tau, 0) e^{-\tau_0 H_{\text{initial}}} | \psi_T \rangle}{\langle \psi_T | e^{-\tau_0 H_{\text{initial}}} U(2\tau, 0) e^{-\tau_0 H_{\text{initial}}} | \psi_T \rangle}. \quad (\text{S2})$$

In numerical calculations, we use Trotter decomposition to discretize imaginary-time propagator into $M = \Theta/\Delta\tau$ (M is integer and Θ is imaginary time) time slices with

$$e^{-\Theta H} = \prod_{m=1}^M [e^{-\Delta\tau H_t} e^{-\Delta\tau H_U} + \mathcal{O}(\Delta\tau^2)], \quad (\text{S3})$$

where H_t and H_U are the hopping term and the interaction term respectively in the Hamiltonian. We choose small enough $\Delta\tau/t \leq 0.05$. To decouple two-body fermion-fermion coupling form of $e^{\Delta\tau H_U}$, we use discrete Hubbard-Stratonovich transformation

$$e^{-\frac{\Delta\tau U}{2}(n_{i\uparrow} + n_{i\downarrow} - 1)^2} = \sum_{l=\pm 1, \pm 2} \gamma(l) e^{i\sqrt{\frac{\Delta\tau U}{2}} \eta(l)(n_{i\uparrow} + n_{i\downarrow} - 1)}, \quad (\text{S4})$$

$$e^{-\frac{\Delta\tau V}{2}(n_i + n_j - 1)^2} = \sum_{l=\pm 1, \pm 2} \gamma(l) e^{i\sqrt{\frac{\Delta\tau V}{2}} \eta(l)(n_i + n_j - 1)}, \quad (\text{S5})$$

to obtain one-body fermion-auxiliary field coupling. Here, we introduce four-component space-time local auxiliary fields $\gamma(\pm 1) = 1 + \sqrt{6}/3$, $\gamma(\pm 2) = 1 - \sqrt{6}/3$, $\eta(\pm 1) = \pm\sqrt{2(3 - \sqrt{6})}$, $\eta(\pm 2) = \pm\sqrt{2(3 + \sqrt{6})}$, and use DQMC for importance sampling over these space-time configurations. Next, we elaborate on how DQMC numerically calculates the sampling weight.

Taking Hubbard interaction as an example, for each imaginary time and each position of the interaction, we employ Hubbard-Stratonovich transformation as in Eq. (S4). This means that we introduce an auxiliary field in $d + 1$ dimensions. As a result, the imaginary-time propagator can be fully expressed using single-particle operators. This allows us to represent it in the following quadratic form of fermion operators:

$$e^{-\Theta H} \equiv \sum_{\mathbf{c}} e^{-\Theta H_{\mathbf{c}}} = \sum_{\mathbf{c}} A_{\mathbf{c}} \prod_{m=1}^M e^{\vec{c}^t T \vec{c}} e^{\vec{c}^t V_{\mathbf{c}(m)} \vec{c}}, \quad (\text{S6})$$

where $\sum_{\mathbf{c}}$ denotes the summation over all space-time configurations of the auxiliary field. Considering that each local component of the auxiliary field has 4 possible values, the summation comprises up to 4^{MN} terms, where N represents the number of spatial degrees of freedom. $H_{\mathbf{c}}$ denotes the decoupled configuration Hamiltonian, while T and $V_{\mathbf{c}(m)}$ are the resulting quadratic coefficient matrices from the rearrangement, and $A_{\mathbf{c}}$ is the coefficient. Both $V_{\mathbf{c}(m)}$ and $A_{\mathbf{c}}$ depend on the auxiliary field configuration. The complete form of the evolution operator has been presented above. Next, we consider expressing the trial wave function. We use a DSM initial state for trial wave function, which is a direct product state, and numerically it can be written as the following Slater determinant:

$$|\psi_T\rangle = \bigotimes_{n_e=1}^{N_e} \left[\left(\sum_x c_x^\dagger P_{x,n_e} \right) |0\rangle \right] = \bigotimes_{n_e=1}^{N_e} \left[(\bar{c}^\dagger P)_{n_e} |0\rangle \right], \quad (\text{S7})$$

where N_e denotes the number of electrons. This implies that the trial wave function is a direct product of N_e fermion single-particle wave functions. The index x denotes the degree of freedom of the electron, including spatial degrees of freedom, spin degrees of freedom, etc. The matrix element P_{x,n_e} represents the probability amplitude of the n_e th electron on the x th degree of freedom. Note that the imaginary-time propagator $e^{-\Theta H_{\mathbf{c}}}$ is essentially the Boltzmann weight factor of the auxiliary field configuration in statistical mechanics. According to Eqs. (S6) and (S7), the partition function of the auxiliary field configuration can be expressed as:

$$Z = \sum_{\mathbf{c}} \langle \psi_T | e^{-\Theta H_{\mathbf{c}}} | \psi_T \rangle = \sum_{\mathbf{c}} A_{\mathbf{c}} \det [P^\dagger B_{\mathbf{c}}(\Theta, 0) P]. \quad (\text{S8})$$

Here, we use $B_{\mathbf{c}}$ to represent the exponential of the quadratic coefficient matrix:

$$B_{\mathbf{c}}(\tau_2, \tau_1) \equiv \prod_{m=\tau_1/\Delta\tau}^{\tau_2/\Delta\tau} e^T e^{V_{\mathbf{c}(m)}}. \quad (\text{S9})$$

The expression on the right side of Eq. (S8) has integrated out the fermion operators, replacing the Grassmann numbers and fermion statistics with a determinant representation which is computationally tractable. All matrix operations can be performed directly on a computer.

Ultimately, our Monte Carlo sampling is conducted over space-time configurations. Numerically, the weight of a space-time configuration is $A_{\mathbf{c}} \det [P^\dagger B_{\mathbf{c}}(\Theta, 0) P]$. Following the classical Markov importance sampling method, we continuously make tentative flips to the local components of this $d+1$ dimensional auxiliary field. We then employ the Metropolis algorithm to calculate the probability of accepting these changes based on the ratio of configuration weights before and after the flip. Specifically, we need to compute the following weight ratio:

$$R_{\mathbf{c}'\mathbf{c}} \equiv \frac{A_{\mathbf{c}'} \det [P^\dagger B_{\mathbf{c}'}(\Theta, 0) P]}{A_{\mathbf{c}} \det [P^\dagger B_{\mathbf{c}}(\Theta, 0) P]}, \quad (\text{S10})$$

where \mathbf{c}' represents the flipped configuration and \mathbf{c} represents the original configuration. In fact, we do not need to compute the weights of the two configurations separately. This is because the flipping we perform is localized in space-time, so

$$B_{\mathbf{c}'}(\Theta, 0) = B_{\mathbf{c}}(\Theta, \zeta) (\mathbf{1} + \Delta_{\mathbf{c}'\mathbf{c}}) B_{\mathbf{c}}(\zeta, 0). \quad (\text{S11})$$

Here, $\Delta_{\mathbf{c}'\mathbf{c}}$ is a highly sparse matrix, where only the matrix elements corresponding to the degrees of freedom involved in the local auxiliary field flipping are non-zero. Thus, the ratio of the two determinants can be expressed as:

$$\frac{\det [P^\dagger B_{\mathbf{c}'}(\Theta, 0) P]}{\det [P^\dagger B_{\mathbf{c}}(\Theta, 0) P]} = \det \left\{ \mathbf{1} + \Delta_{\mathbf{c}'\mathbf{c}} B_{\mathbf{c}}(\zeta, 0) P [P^\dagger B_{\mathbf{c}}(\Theta, 0) P]^{-1} P^\dagger B_{\mathbf{c}}(\Theta, \zeta) \right\}. \quad (\text{S12})$$

Due to the sparsity of $\Delta_{\mathbf{c}'\mathbf{c}}$, the determinant on the right side of the above equation only requires consideration of a few degrees of freedom involved in the flipping during computations.

In DQMC, to compute the physical observables, we only need to statistically analyze the configurational observable $\langle O(\tau) \rangle_{\mathbf{c}}$.

$$\langle O(\tau) \rangle = \sum_{\mathbf{c}} \text{Pr}_{\mathbf{c}} \langle O(\tau) \rangle_{\mathbf{c}} + \mathcal{O}(\Delta\tau^2), \quad (\text{S13})$$

where Pr_c represents the configuration probability,

$$\text{Pr}_c = \frac{1}{Z} A_c \det [P^\dagger B_c(2\tau + \tau_0, 0)P], \quad (\text{S14})$$

$$\langle O(\tau) \rangle_c = \frac{\langle \psi_0 | U_c(2\tau, \tau) O U_c(\tau, 0) | \psi_0 \rangle}{\langle \psi_0 | U_c(2\tau, 0) | \psi_0 \rangle} = \frac{\langle \psi_T | e^{-\tau_0 H_{\text{initial},c}} U_c(2\tau, \tau) O U_c(\tau, 0) e^{-\tau_0 H_{\text{initial},c}} | \psi_T \rangle}{\langle \psi_T | e^{-\tau_0 H_{\text{initial},c}} U_c(2\tau, 0) e^{-\tau_0 H_{\text{initial},c}} | \psi_T \rangle}. \quad (\text{S15})$$

Since we employ importance sampling, the sampling frequency is proportional to the configuration probability. Ultimately, when calculating the observable, we simply take the average over the sampled configurational observables. If the observable is a single-particle operator, meaning it can be expressed as a quadratic form of fermion operators, then one can integrate out the fermion degrees of freedom in a manner similar to Eq. (S8) and numerically compute using determinants. For observables of four-fermion operators or higher, we compute using the fermion equal-time Green's function based on Wick's theorem. After numerically integrating out the fermion degrees of freedom, the fermion equal-time Green's function can be expressed using the following matrix element:

$$\langle c_{x_1}^\dagger c_{x_2} \rangle_c = \left\{ B_c \left(\frac{\Theta}{2}, 0 \right) P [P^\dagger B_c(\Theta, 0)P]^{-1} P^\dagger B_c \left(\Theta, \frac{\Theta}{2} \right) \right\}_{x_1, x_2}. \quad (\text{S16})$$

RESULTS OF DIMENSIONLESS QUANTITY

In the main text, we only present dynamic results of the square of the order parameter m^2 . Here, we supplement the results of a dimensionless quantity correlation ratio defined as [179]:

$$R_S \equiv 1 - S(\Delta\mathbf{q})/S(\mathbf{0}), \quad (\text{S17})$$

where $\Delta\mathbf{q}$ is the minimum lattice momentum and $S(\mathbf{q})$ is the structure factor.

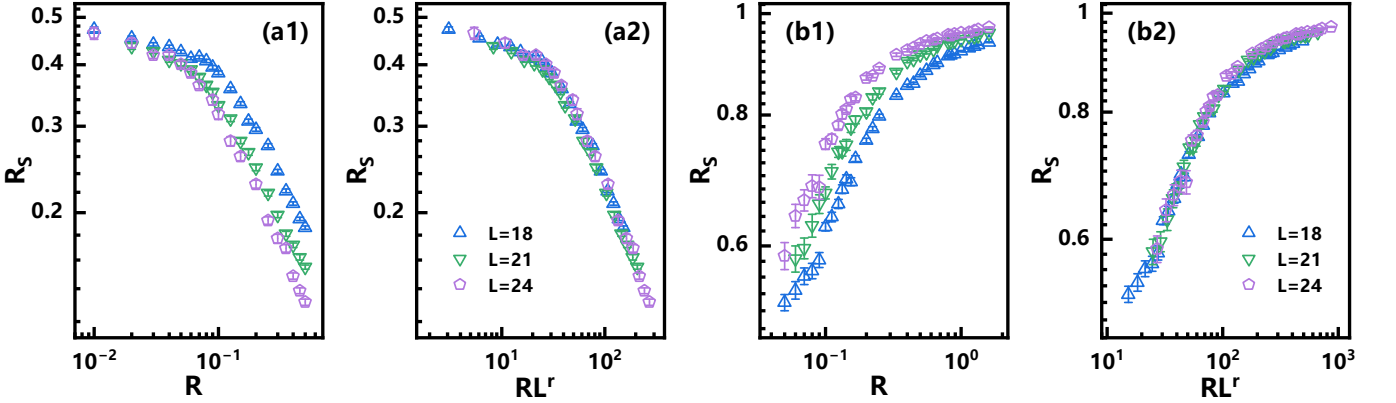


FIG. S1. Log-log plots of R_S versus R for different L driven to $U_c = 3.85$, for model (1). (a1) displays the results driven from the DSM phase. (a2) shows rescaling is applied to the horizontal axis of (a1). (b1) displays the results driven from the AFM phase. (b2) shows rescaling is applied to the horizontal axis of (b1).

For model (1), $S(\mathbf{q})$ is the antiferromagnetic structure factor:

$$S(\mathbf{q})_{\text{AFM}} = \frac{1}{L^{2d}} \sum_{i,j} e^{i\mathbf{q}\cdot(\mathbf{r}_i - \mathbf{r}_j)} \langle S_i^z S_j^z \rangle, \quad (\text{S18})$$

where S_i^z is the staggered magnetization operator defined as $S_i^z \equiv \vec{c}_{i,A}^\dagger \sigma^z \vec{c}_{i,A} - \vec{c}_{i,B}^\dagger \sigma^z \vec{c}_{i,B}$ with i characterizes cells and $\vec{c}^\dagger \equiv (c_\uparrow^\dagger, c_\downarrow^\dagger)$.

For model (4), $S(\mathbf{q})$ is the charge-density-wave structure factor:

$$S(\mathbf{q})_{\text{CDW}} = \frac{1}{L^{2d}} \sum_{i,j} e^{i\mathbf{q}\cdot(\mathbf{r}_i - \mathbf{r}_j)} \langle n_i n_j \rangle, \quad (\text{S19})$$

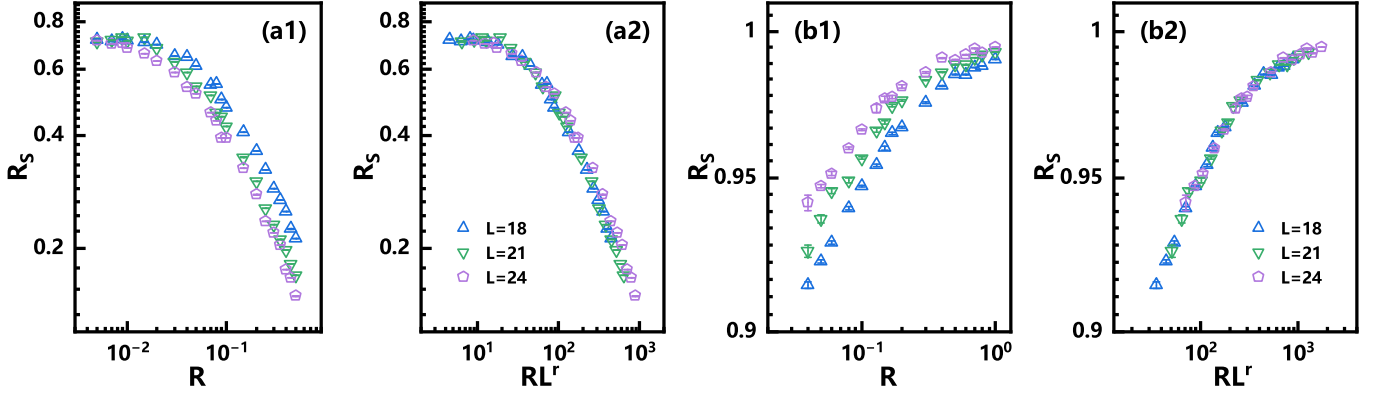


FIG. S2. Log-log plots of R_S versus R for different L driven to $V_c = 1.355$, for model (4). (a1) displays the results driven from the DSM phase. (a2) shows rescaling is applied to the horizontal axis of (a1). (b1) displays the results driven from the CDW phase. (b2) shows rescaling is applied to the horizontal axis of (b1).

where $n_i \equiv n_{i,A} - n_{i,B}$ with $n_{i,A}$ being the electron number operator defined as $n_{i,A} \equiv c_{i,A}^\dagger c_{i,A}$.

According to the scaling analysis in the main text, as a dimensionless variable, R_S in the driven process obeys the following dynamic scaling form:

$$R_S(g, R, L) = f(RL^r, gL^{1/\nu}), \quad (\text{S20})$$

which indicates that (S20) at $g = 0$ can be converted to $R_S = f(RL^r)$.

As shown in Fig. S1(a2)(b2) and Fig. S2(a2)(b2), we find that the rescaled curves all collapse well. These results not only confirm (S20) at $g = 0$, but also support the conclusions we draw in the main text.